Chem

CellPress

Article

Extremely Hydrophobic POPs to Access Highly Porous Storage Media and Capturing Agent for Organic Vapors

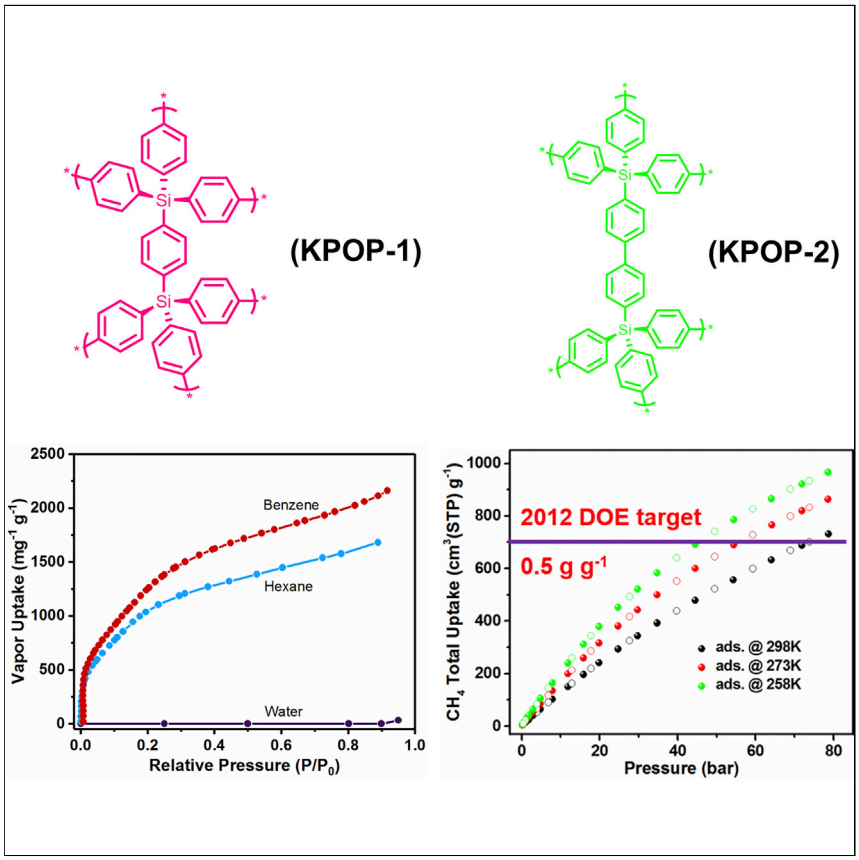

Eddaoudi and co-workers implemented the molecular-building-block strategy to isolate three porous organic polymers (POPs), namely KPOP-1, KPOP-2, and KPOP-3 (KPOP = KAUST's POP), exhibiting high surface areas. Impressively, the methane uptake of KPOP-2 at 298 K and 80 bar is 0.515 g g^{-1}, surpassing the gravimetric 2012 Department of Energy target for onboard CH_4 storage. Interestingly, KPOP-1 and KPOP-2 showed high hydrophobic behavior and high organic vapor uptakes, ranking them as promising candidates for the removal of volatile organic compounds at atmospheric conditions.

Jiangtao Jia, Zhijie Chen, Hao Jiang, ..., Justyna Czaban-Jóźwiak, Mohamed Rachid Tchalala, Mohamed Eddaoudi

mohamed.eddaoudi@kaust.edu.sa

HIGHLIGHTS

Highly porous organic frameworks with hypothetically approximated topologies

KPOP-2 surpasses the gravimetric 2012 DOE target for onboard CH_4 storage

KPOP-2 shows exclusive potential for stationary CH_4 storage

KPOP-1 shows exceptional performances for capturing VOCs

Jia et al., Chem 5, 1–12
January 10, 2019
https://doi.org/10.1016/j.chempr.2018.10.005

Please cite this article in press as: Jia et al., Extremely Hydrophobic POPs to Access Highly Porous Storage Media and Capturing Agent for Organic Vapors, Chem (2018), https://doi.org/10.1016/j.chempr.2018.10.005

Chem

CellPress

Article

Extremely Hydrophobic POPs to Access Highly Porous Storage Media and Capturing Agent for Organic Vapors

Jiangtao Jia,[1] Zhijie Chen,[1] Hao Jiang,[1] Youssef Belmabkhout,[1] Georges Mouchaham,[1] Himanshu Aggarwal,[1] Karim Adil,[1] Edy Abou-Hamad,[2] Justyna Czaban-Jóźwiak,[1] Mohamed Rachid Tchalala,[1] and Mohamed Eddaoudi[1,3,*]

SUMMARY

Porous organic polymers (POPs) with high surface areas (especially more than 5,000 m^2 g^{-1}) are still quite rare. In this work, we implemented the molecular-building-block strategy to isolate three POPs, namely KPOP-1, KPOP-2, and KPOP-3 (KPOP = KAUST's POP), and hypothetically predicted the structures of the three KPOPs. KPOP-1 and KPOP-2 exhibit high specific BET surface areas (ca. 5,120 and 5,730 m^2 g^{-1}) and display outstanding gravimetric methane storage properties. Remarkably, the methane uptake of KPOP-2 at 298 K and 80 bar is 0.515 g g^{-1}, surpassing the gravimetric 2012 Department of Energy target for onboard CH_4 storage, and KPOP-2 shows the exclusive potential for stationary CH_4 storage. Interestingly, KPOP-1 and KPOP-2 show extremely hydrophobic behavior combined with high organic vapor uptakes, a desirable feature enabling effective capturing of volatile organic compounds at room temperature.

INTRODUCTION

The enduring fast growth of the global economy steered a greater than previous demand for the consumption of fossil fuels such as petroleum, in turn provoking the remarkable and uncontrollable escalation of CO_2 emission, ground-level air pollution, and climate change. Natural gas (NG) with methane as the main component offers a distinct environmentally sustainable alternative, in the short to medium term, to substitute the conventional petroleum-based fuels and significantly reduce the adverse emissions responsible for climate change.[1,2] Nevertheless, the transportation and storage operations of NG using compression under high pressure are costly and require numerous demanding preventive measures. Adsorbed NG (ANG) storage systems encompassing porous materials in the storage tanks offer great potential to reduce the storage pressure and increase the energy density.[3] For this purpose, the appropriate adsorbent material should have high porosity and high thermal stability, and offer effective mode for regeneration and recycling while addressing the US Department of Energy (DOE) released new gravimetric CH_4 storage target of 50 wt % in 2012[3,4] for onboard applications. It is noteworthy that the gravimetric CH_4 storage is the only driving parameter for a stationary ANG system because of the less constrained requirements for space and volume. To achieve the ultimate goal in enhancing gravimetric storage, the most important metrics for porous materials are high specific surface area and large pore volume.[5]

The Bigger Picture

The ability to develop advanced highly porous storage and separating agents with the requisite properties, affording exceptional gravimetric CH_4 uptake and aromatics combined with non-competitive adsorption of water vapor, is of prime importance. Successful future implementation of these disruptive adsorptive technologies offers great potential to address various United Nations sustainable development goals pertaining to clean, reliable, and sustainable energy and prosperous health. Herein, we unveil three highly porous organic frameworks, KPOP-1, KPOP-2, and KPOP-3 (KPOP stands for KAUST's porous organic polymer), which display outstanding properties for CH_4 storage and the capture of volatile organic compounds to address many critical societal and industrial challenges.

Please cite this article in press as: Jia et al., Extremely Hydrophobic POPs to Access Highly Porous Storage Media and Capturing Agent for Organic Vapors, Chem (2018), https://doi.org/10.1016/j.chempr.2018.10.005

The exploration of highly porous materials, and their associated potential applications, has been an active area of research in academia and industry alike. During the last two decades, metal-organic frameworks (MOFs) with ultra-high surface area such as MOF-210,[6] NU-110,[7] and Al-soc-MOF-1[8] have been vigorously explored. However, because of the trade-off between high porosity and stability, most of the highly porous MOFs showed a lessened chemical stability as the surface area increased and most of them required impractical activation methods such as supercritical CO_2.[9] These MOFs usually cannot preserve their structures under highly acidic or basic conditions, thus limiting their wide industrial applications. Only recently, Eddaoudi et al. unveiled a unique isostructural **soc**-MOF based on Cr satisfying the challenging high porosity-stability trade-off.[10]

More recently, porous organic polymers (POPs),[11–14] offering superior stability to MOFs because of their robust covalent bonds, have attracted considerable attention for gas storage[15] as well as for separation.[16] Irreversible and fast reaction approaches are usually applied to synthesize POPs. These methodologies lead often to amorphous polymers with highly heterogeneous structures. As POP structural features remain usually unknown, it is very challenging to design and construct POPs with high surface areas.[17–20] Only very few examples of POPs have been reported with ultra-high surface areas comparable with MOFs. For example, partially crystalline PAF-1[21] possesses an estimated BET (BET = Brunauer-Emmett-Teller) surface area[22] of ca. 5,600 $m^2\ g^{-1}$. Another reported POP (PPN-4)[23] exhibits an even higher BET specific surface area of around 6,400 $m^2\ g^{-1}$. The two aforementioned POPs were both synthesized using 4-connected (4-c) building blocks in order to mimic the hypothetical diamond (**dia**) structure. Nevertheless, the use of building blocks with higher connectivity, i.e., a higher degree of predictability, is of significant importance and rarely explored.

The molecular building block (MBB) approach[24,25] decidedly permits access to POPs by the assembly of judiciously preselected organic building blocks that code geometrical information of targeted underlying nets. Although POPs assembled from 3-connected (3-c) and 4-c MBBs[20,26] have been widely explored, 6-c MBBs[27,28] have rarely been studied in constructing 3D POPs, owing to their complex conformation and the difficulty to predict obtained structures compared with 3-c and 4-c MBBs. Herein, three 6-c MBBs (Figures 1 and S26–S40), i.e., 1,4-bis(tris(4-bromophenyl)silyl)-benzene (MBB-1), 4,4′-bis(tris(4-bromophenyl)silyl)-1,1′-biphenyl (MBB-2), and 5′-(3,5-diethynylphenyl)-3,3″,5,5″-tetraethynyl-2′,4′,6′-trimethyl-1,1′:3′,1″-terphenyl (MBB-3), were designed and synthesized as precursors to deliberately assemble the targeted 3D POPs. Using these MBBs, three POPs, namely KPOP-1, KPOP-2, and KPOP-3 (KPOP = KAUST [King Abdullah University of Science and Technology] POP), were synthesized and show high specific BET surface areas of 5,120, 5,730, and 2,620 $m^2\ g^{-1}$, respectively. Thanks to their ultra-high porosity, the reported POPs displayed records of gravimetric uptakes for CH_4, CO_2, and O_2. Interestingly, KPOP-1 and -2 also show an extremely hydrophobic behavior and an exceptional adsorption of large amounts of organic vapors, positioning them as very promising adsorbent materials for the capture of volatile organic compounds (VOCs).

RESULTS AND DISCUSSION

The Reticular Chemistry Structure Resource (RCSR) lists the nets with underlying topologies **acs**, **bcs**, **crs**, **lcy**, and **pcu** (Figure S1) as the five edge-transitive nets constructed by one type of 6-c building units with trigonal prism, octahedral, or trigonal anti-prism geometry.[29,30] On the basis of the MBB conformation analysis,

[1]Functional Materials Design, Discovery and Development Research Group, Advanced Membranes and Porous Materials Center, Division of Physical Sciences and Engineering, King Abdullah University of Science and Technology, Thuwal 23955-6900, Saudi Arabia

[2]King Abdullah University of Science and Technology, Core Labs, Thuwal 23955-6900, Saudi Arabia

[3]Lead Contact

*Correspondence: mohamed.eddaoudi@kaust.edu.sa

https://doi.org/10.1016/j.chempr.2018.10.005

Please cite this article in press as: Jia et al., Extremely Hydrophobic POPs to Access Highly Porous Storage Media and Capturing Agent for Organic Vapors, Chem (2018), https://doi.org/10.1016/j.chempr.2018.10.005

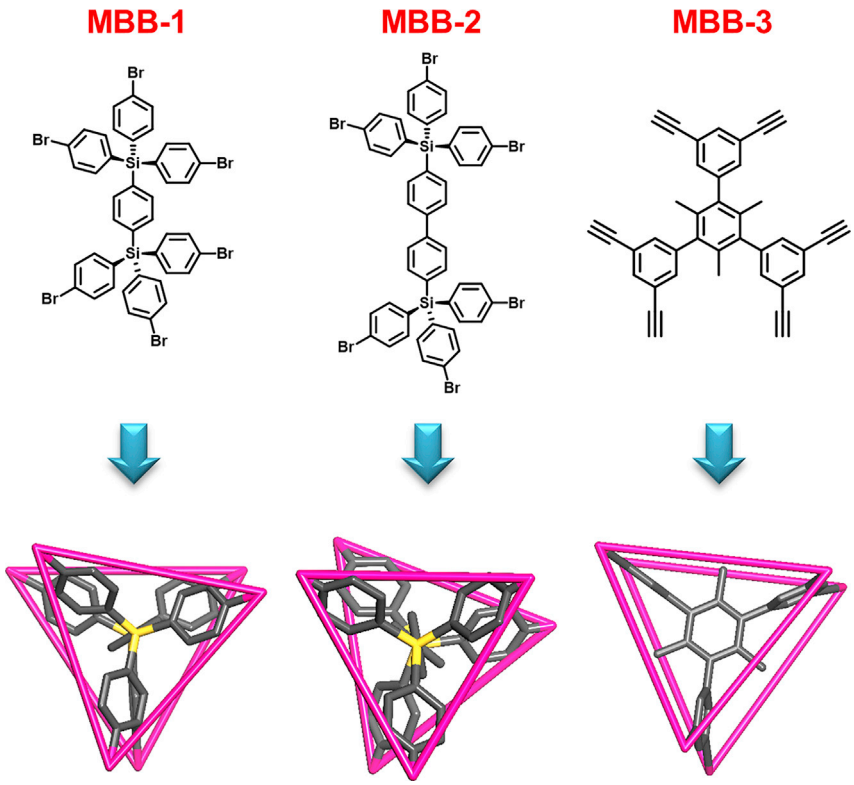

Figure 1. Geometrically Optimized Conformations of MBB-1, MBB-2, and MBB-3 by Materials Studio 8.0 Software with the Forcite Module

Hydrogen atoms are omitted for clarity. Black, carbon atoms; yellow, silicon atoms.

it can be expected that MBB-1 and MBB-2 with twisted trigonal prism conformations offer great prospective to construct frameworks with **acs**, **bcs**, **crs**, **lcy**, or **pcu** underlying topologies. MBB-1 and MBB-2 can afford two possible conformations, namely the trigonal prism or the trigonal anti-prism, by the phenyl rings rotating. MBB-3 may form a structure with the **acs** underlying net because **acs** is the only edge-transitive net based on linking trigonal prism building units. Replacing the nodes of each net with MBB-1 and MBB-2, five POP structures can be simulated. However, after geometry optimization by forcite field in Material Studio 8.0, it was found that only **acs**, **pcu**, and **lcy** nets are theoretically plausible and/or suitable for MBB-1 and MBB-2, whereas the chemical bonds in POPs based on **crs** and **bcs** nets are unreasonable. With the same method, a structure showing reasonable chemical bonds based on the **acs** net and MBB-3 was also simulated (Figure 2). From the calculated results, it was found that all KPOPs based on **acs**, **pcu**, and **lcy** nets have high theoretical specific BET surface areas (Table S1), thus prompting our interest to assemble them experimentally.

Gratifyingly, we successfully synthesized KPOP-1, KPOP-2, and KPOP-3 by employing MBB-1, MBB-2, and MBB-3, respectively. Indeed, Yamamoto coupling was applied to synthesize KPOP-1 and KPOP-2, resulting in white powder-like materials that are insoluble in conventional organic solvents (i.e., dimethylformamide [DMF], tetrahydrofuran [THF], and dichloromethane). Infrared spectra of KPOP-1 and KPOP-2 revealed the absence of the signature C–Br bond stretching peak at 1,065 cm^{-1}, suggesting the successful coupling of the monomers (Figures S6 and S7). Energy-dispersive X-ray spectroscopy (EDX) data (Figure S3) showed there

Please cite this article in press as: Jia et al., Extremely Hydrophobic POPs to Access Highly Porous Storage Media and Capturing Agent for Organic Vapors, Chem (2018), https://doi.org/10.1016/j.chempr.2018.10.005

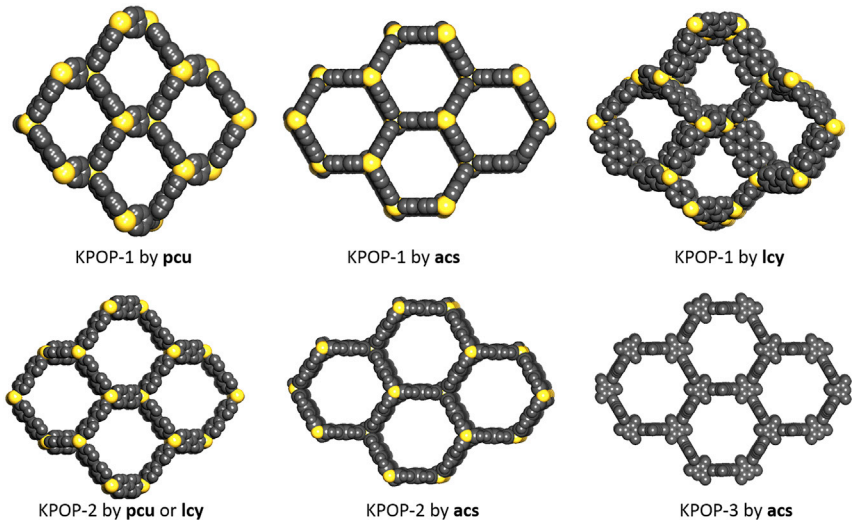

Figure 2. Simulated Structures of Idealized Crystalline Forms of KPOP-1, KPOP-2, and KPOP-3
Hydrogen atoms are omitted for clarity. Black, carbon atoms; yellow, silicon atoms.

are almost no Br residue signals, attributable to the high complement of polymerization and the conversion of the ending -Br to -H during quenching of the nickel coordinated complexes by hydrochloric acid.[31] The scanning electron microscopy (SEM) images (Figure S2) of KPOP-1 and KPOP-2 showed aggregated particles with the size ranging from 200 to 300 nm. It must be noted that the Yamamoto coupling reaction can form polymers with partial crystallinity.[21,23] Consequently, powder X-ray diffraction (PXRD) studies were performed to assess the crystallinity of KPOP-1 and KPOP-2 (Figure S5). The two PXRD patterns showed quite broad peaks showing that both solids are mainly amorphous. In addition, crystal lattices could not be found from the high-resolution transmission electron microscopy (HRTEM) images, probably because of the weak crystallinity (Figure S4).

MBB-3 was designed and synthesized for the first time and used to synthesize KPOP-3 via Eglinton coupling. Reacting MBB-3 with $Cu(OAc)_2$ in pyridine yielded KPOP-3 as a brown solid that is insoluble in most of the conventional organic solvents. Infrared spectra of KPOP-3 (Figure S8) did not reveal any peak at 3,280 cm^{-1} (the characteristic peak of alkyne's C–H bond stretching), attesting to the completion of the reaction. SEM images (Figure S2) showed very small aggregated particles and PXRD patterns (Figure S5) revealed no peaks, indicating no long-range order.

The thermal stability of the three KPOPs was evaluated by performing thermalgravimetric analysis under oxygen atmosphere (Figure S9). KPOP-2 has a higher decomposition temperature (around 440°C) than KPOP-1 (around 370°C), even though they both have very similar compositions. This could be because KPOP-2 has a relatively more stable 3D structure than KPOP-1. After 600°C, KPOP-1 and KPOP-2 decompose to form silica. KPOP-3 has the lowest decomposition temperature among the three KPOPs owing to the active carbon triple bond. From 150°C, KPOP-3's weight increases by about 2% perhaps because of the oxidation of the carbon triple bond, and the main framework starts to decompose around 200°C. After 500°C, about 4% weight residue was observed. This may be attributed to the formation of CuO from plausibly entrapped $Cu(OAc)_2$ catalyst in the pores of KPOP-3. The presence of Cu residues was also confirmed by the EDX analysis of KPOP-3 (Figure S3).

Please cite this article in press as: Jia et al., Extremely Hydrophobic POPs to Access Highly Porous Storage Media and Capturing Agent for Organic Vapors, Chem (2018), https://doi.org/10.1016/j.chempr.2018.10.005

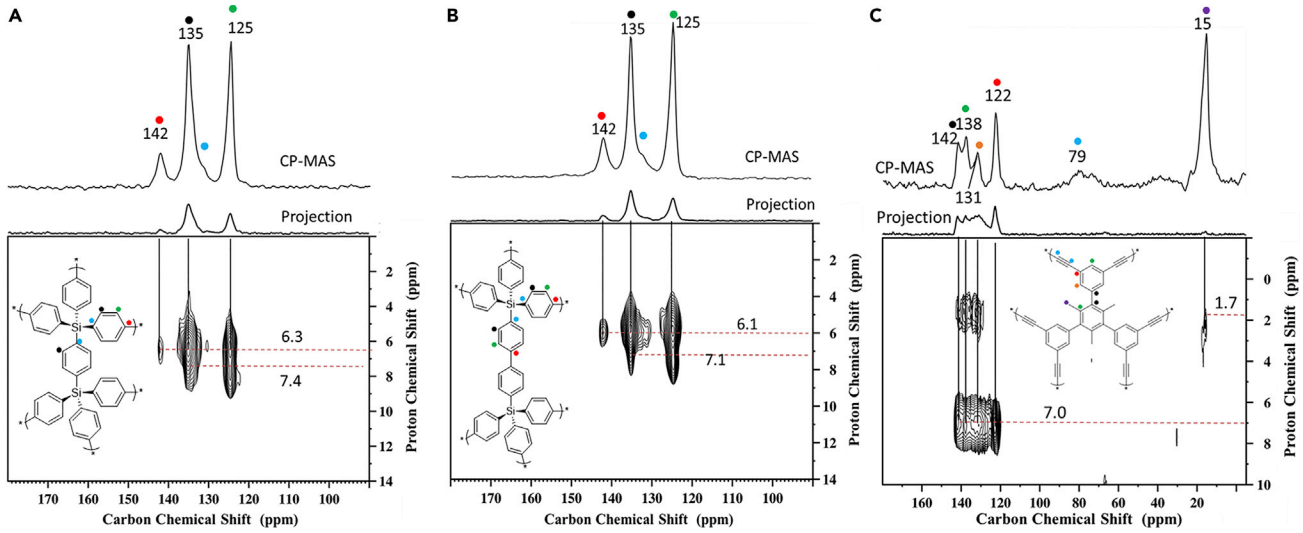

Figure 3. ^{13}C CP MAS and 2D ^{1}H-^{13}C HETCOR NMR
KPOP-1 (A), KPOP-2 (B), and KPOP-3 (C).

To gain further insights into the chemical structures of the POPs, we performed multinuclear (^{1}H, ^{13}C, and ^{29}Si) solid-state nuclear magnetic resonance (SS-NMR) spectroscopy studies on KPOP-1, KPOP-2, and KPOP-3. Figure 3A illustrates the ^{13}C cross-polarization magic-angle spinning (CP MAS) and 2D ^{1}H-^{13}C heteronuclear correlation spectroscopy (HETCOR) NMR for KPOP-1. The signals at δ = 142, 135, 131, and 125 ppm indicate the presence of four different aromatic carbon atoms in KPOP-1 clearly assigned with different colored labels. The ^{1}H MAS NMR shows a merged peak at δ = 7.0 ppm, which can be attributed to the aromatic hydrogen peak in KPOP-1 (Figure S10). The 2D ^{1}H-^{13}C HETCOR NMR spectrum of KPOP-1shows different aromatic protons at 6.3 and 7.4 ppm that reveals correlations with the different aromatic carbons. Strong correlations are shown for black- and green-labeled carbon and protons, indicating the direct bonding that is reasonable in the structure of KPOP-1. The weak correlations of blue- and red-labeled carbon atoms with protons demonstrate that there is a long-distance contact. KPOP-2 shows similar ^{13}C CP MAS spectra with KPOP-1 with the existence of signals at δ = 142, 135, 131, and 125 ppm associated with aromatic carbon atoms. The ^{1}H MAS NMR also shows a merged proton peak at δ = 7.0 ppm corresponding to the aromatic protons (Figure S12). The 2D NMR ^{1}H-^{13}C HETCOR NMR spectrum reveals that black- and green-labeled carbon atoms are directly connected to proton atoms, and the other two carbon atoms have long-distance relation with the proton. Both KPOP-1 and KPOP-2 have peak at δ = −14 ppm in ^{29}Si CP MAS NMR, confirming the presence of silicon atoms (Figures S11 and S13).

KPOP-3 exhibits quite different composition in comparison with KPOP-1 and KPOP-2, as clearly evidenced from the NMR spectrum. The ^{1}H MAS NMR spectrum displays two signals at 1.7 and 7.0 ppm attributed to the methyl and aromatic protons, respectively (Figure S14). The ^{13}C CP MAS NMR spectrum (Figure 3C) displays different signals at 15, 79, 122, 131, 138, and 142 ppm. Additionally, the 2D ^{1}H-^{13}C HETCOR NMR spectrum (Figure 3C) shows a correlation between the methyl protons at 1.7 ppm and their corresponding carbon atoms at 15 ppm. Furthermore, the peak at 79 ppm shows no correlations with any proton signal assigned to acetylene carbon atoms. The distribution of aromatic carbon atom signals between

Please cite this article in press as: Jia et al., Extremely Hydrophobic POPs to Access Highly Porous Storage Media and Capturing Agent for Organic Vapors, Chem (2018), https://doi.org/10.1016/j.chempr.2018.10.005

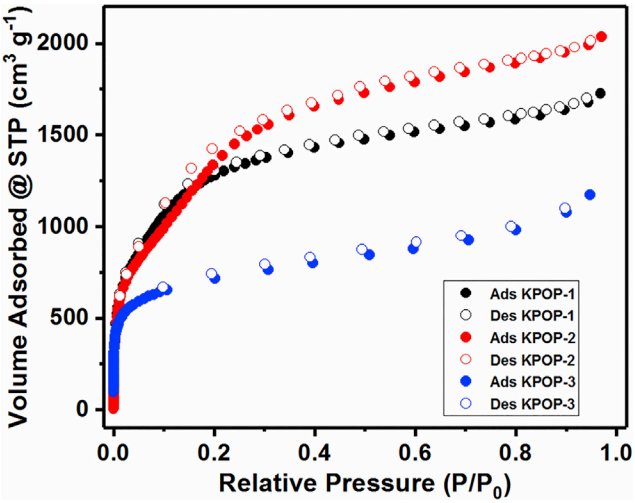

Figure 4. N_2 Isotherms at 77 K
Black, KPOP-1; red, KPOP-2, blue, KPOP-3.

122 and 142 ppm shows a strong correlation with aromatic proton signal at 7 ppm, confirming their relationship in the predicted structure.

To attest the expected high porosity of KPOPs, we first explored their permanent porosity by N_2 sorption studies at 77 K (Figure 4). The N_2 adsorption isotherms showed that KPOP-1, KPOP-2, and KPOP-3 have very high specific BET surface areas of ca. 5,120, 5,730, and 2,620 $m^2\ g^{-1}$, respectively (Figures S15, S17, and S19). The single point pore volumes at P/P_0 = 0.95 were found to be 2.60, 3.09, and 1.67 $cm^3 g^{-1}$, respectively. The pore-size distributions determined via density functional theory afford the approximation of the possible pore size of the KPOPs (Figures S16, S18, and S20). It was found that the lowest and highest average pore sizes are 1.4 and 2.1 nm, respectively, for KPOP-1 and 1.5 and 2.5 nm, respectively, for KPOP-2; KPOP-3 displayed an average pore size at ca. 1.7 nm. According to the simulated possible structures of KPOPs, the experimental specific BET surface area and pore volumes of KPOP-1 and KPOP-2 corroborate with the simulated ones. In the simulated structures, the calculated BET surface areas of KPOP-1 and KPOP-2 are around 5,300 and 5,900 $m^2\ g^{-1}$, respectively, and the calculated pore dimensions are both around 1.4 nm. As a result of the plausible amorphous structures and vague side reactions, KPOP-1 and KPOP-2 have somewhat lower experimental BET surface areas and larger pore size than the simulated structures.

Interestingly, KPOP-2 has a slightly lower specific BET surface area than PNN-4 (6,461 $m^2\ g^{-1}$)[23] but a similar one to PAF-1 (5,600 $m^2\ g^{-1}$),[21] the only two reported POPs displaying ultra-high specific BET surface areas (>5,000 $m^2\ g^{-1}$). However, the pore volume of KPOP-2 is slightly larger than those of PNN-4 and PAF-1 mainly because of its associated larger pore size. Accordingly, KPOP-2 is expected to offer greater adsorption and storage performances than the compounds cited above. KPOP-3 displays lower specific BET but remains high among the POPs constructed via Eglinton coupling reaction.[32]

The exceptional porosity features for the aforementioned KPOP compounds encouraged us to further investigate their associated high-pressure sorption performance for different gases, i.e., methane (CH_4), oxygen (O_2), and carbon dioxide

Please cite this article in press as: Jia et al., Extremely Hydrophobic POPs to Access Highly Porous Storage Media and Capturing Agent for Organic Vapors, Chem (2018), https://doi.org/10.1016/j.chempr.2018.10.005

Table 1. Summary of the Porous Materials with High Absolute Gravimetric Methane Uptake at 298 K

Materials	Methane Uptake ($g\ g^{-1}$)		Working Capacity ($g\ g^{-1}$)		Reference
	80 bar	35 bar	5–80 bar	5–35 bar	
KPOP-2	0.515	0.277	0.469	0.232	this work
PPN-4	ND	0.274	ND	0.231	Li et al.,[1] Yuan et al.[23]
MOF-210	0.476	0.238	0.431	0.193	Furukawa et al.[6]
Al-soc-MOF-1	0.475	0.257	0.425	0.207	Alezi et al.[8]
KPOP-1	0.450	0.255	0.406	0.211	this work
PAF-1	0.400	0.229	0.357	0.186	Bracco et al.[33]
Nu-111	ND	0.241	ND	0.194	Peng et al.[34]
COF-102	0.362	0.234	0.32	0.192	Furukawa et al.[35]
AX-21 (active carbon)	0.328	0.254	0.225	0.151	Mason et al.[5]
KPOP-3	0.262	0.161	0.217	0.116	this work

ND, not determined.

(CO_2). The high-pressure CH_4 sorption studies were conducted up to 80 bar and at various temperatures (298, 273, and 258 K).

In the absence of the crystal structure, it is difficult to obtain the theoretical densities of POPs that are further required to estimate the volumetric CH_4 uptake. Therefore, we aimed first to calculate the skeletal density from the adsorption measurements of non-adsorbable gas (helium) at 298 K. The crystal-like particle densities (hypothetical density) of KPOP-1, KPOP-2, and KPOP-3 were then estimated to be ca. 0.310, 0.267, and 0.435 g cm^{-3}, respectively, by combining the skeletal density and the pore volume, which was obtained experimentally from N_2 adsorption isotherm at 77 K (for details of the calculation, see part 8 of the Supplemental Information).[5]

Hence, the volumetric CH_4 uptakes of KPOP-1, KPOP-2, and KPOP-3 at 298 K and 80 bar were estimated to be 195, 192, and 160 $cm^3\ cm^{-3}$, respectively. Because of the lower density of KPOPs than of most MOFs, KPOP-1, KPOP-2, and KPOP-3 showed relatively lower volumetric uptake than benchmark MOF materials such as HKUST-1[4] and Al-soc-MOF-1.[8] However, KPOP-2 showed a high CH_4 gravimetric uptake associated with a very high working capacity surpassing all of the related benchmark materials (Table 1). The measured bulk density was also tested by pressing the POP solid in a measuring syringe. By measuring the weight and the volume of the samples, we estimated bulk densities of KPOP-1, KPOP-2, and KPOP-3 to be 0.204, 0.185, and 0.265 g cm^{-3}, respectively. Accordingly, the volumetric capacities were recalculated as 128, 133, and 97 $cm^3\ cm^{-3}$ at 298 K and 80 bar for KPOP-1, KPOP-2, and KPOP-3, respectively. As expected, the effect of packing led to a lessened volumetric capacity.

The total gravimetric uptakes of KPOP-1, KPOP-2, and KPOP-3 at 298 K and 35 bar are 358, 388, and 226 $cm^3\ g^{-1}$, respectively (Figure 5). Several MOFs, for example, Al-soc-MOF-1,[8] NU-111,[34] and DUT-49,[36] also exhibit outstanding CH_4 uptakes of around 361, 337, and 364 cm^3 (STP) g^{-1}, respectively, under the same conditions, although they show inferior performance to KPOP-2. Moreover, the CH_4 gravimetric uptake of KPOP-2 at 298 K and 35 bar (388 $cm^3\ g^{-1}$) is even higher than the current benchmark POP materials (i.e., PAF-1 [330 $cm^3\ g^{-1}$] and PPN-4 [384 $cm^3\ g^{-1}$]) under

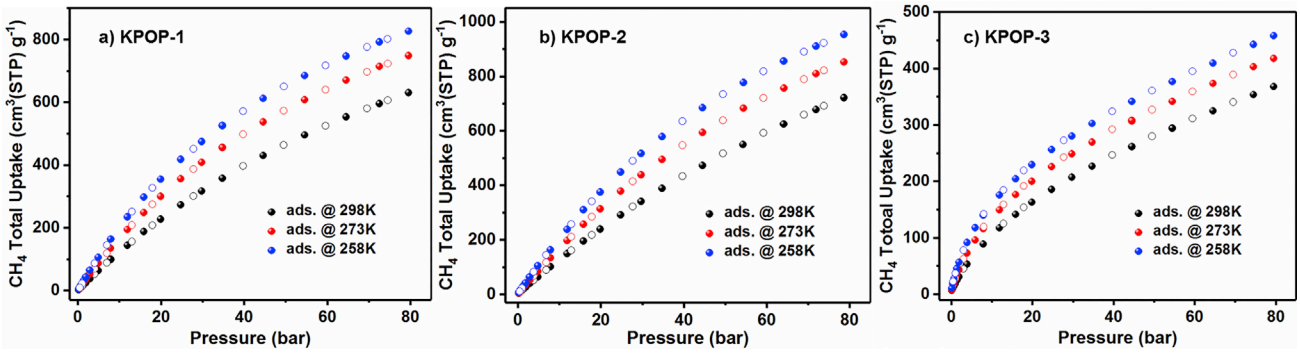

Figure 5. High-Pressure CH_4 Uptake
KPOP-1 (A), KPOP-2 (B), and KPOP-3 (C) at 298, 273, and 258 K, respectively.

the same conditions.[23,33] The higher gravimetric CH_4 uptake of KPOP-2 compared with PPN-4 is attributed to its associated exceptional porosity. At 298 K and 80 bar, KPOP-1, KPOP-2, and KPOP-3 show CH_4 uptakes of 630, 721, and 367 $cm^3\ g^{-1}$, respectively. At lower temperature of 258 K, the CH_4 uptakes of KPOP-1, KPOP-2, and KPOP-3 are much higher and estimated to be 826, 953, and 458 $cm^3\ g^{-1}$, respectively (Figure 5). The CH_4 uptake of KPOP-2 at 80 bar and 298 K is higher than that of most of the reported MOFs. Most importantly, KPOP-2 represents the first porous material capable of addressing the DOE target of 0.5 g g^{-1} at 298 K and 75 bar. The heat of CH_4 adsorption at the lowest CH_4 recorded with reasonable accuracy for KPOP-1, KPOP-2, and KPOP-3 was also calculated to be around 16.6, 16.0, and 19.9 kJ mol^{-1}, respectively (Figures S21–S23).

As shown in Figure S24, at 298 K, 5–35 bar, and 5–80 bar, the working capacity of KPOP-2 is 0.232 and 0.469 g g^{-1}, which is similar to PPN-4 and higher than PAF-1.[23,33] Besides, KPOP-1 showed a high volumetric working capacity of 92 (5–35 bar) and 176 (5–80 bar) $cm^3\ cm^{-3}$ at 298 K, comparable with PPN-4 (92 $cm^3\ cm^{-3}$, 5–35 bar, 298 K).[4,8,23] Interestingly, as the temperature decreases both gravimetric and volumetric working capacities of the KPOPs gradually increase, as already reported for several highly porous MOFs.[8] Table 1 summarizes CH_4 uptakes and working capacities of KPOPs and selected relevant porous materials.

Considering the outstanding performance of KPOP-2 for CH_4 storage, we tested its uptake for CO_2 and O_2 (Figures S25 and S26), another two commodities that need to be stored for specific applications. At 298 K and 25 bar, the absolute gravimetric CO_2 uptake of 1.51 g g^{-1} is higher than PPN-4's, with an uptake of around 1.40 g g^{-1} under the same conditions. At 298 K and 120 bar, the absolute gravimetric O_2 uptake of around 1.02 g g^{-1} is much higher than for the Al-soc-MOF-1 (0.84 g g^{-1}, 298 K, 120 bar) and NU-125 (0.56 g g^{-1}, 140 bar).[8,37] These results indicate that KPOP-2 is also an exceptional solid adsorbent for CO_2 and O_2 storage.

Exhaust VOCs at the workplace or in confined spaces are strongly hazardous to humans and the environment, and in the real world these exhaust VOCs are always mixed with humidity.[38,39] The ideal method of overcoming this problem is to deploy hydrophobic porous materials that can enable the selective removal of VOCs while repelling water. Considering that KPOP-1 and KPOP-2 are highly porous and encompass mainly hydrophobic organic moieties, we decided to evaluate their adsorption properties for some VOCs and water. As illustrated in Figure 6, the benzene uptake of KPOP-1 and KPOP-2 is as high as 2.2 and 2.6 $g^{-1}\ g^{-1}$ (25°C,

Please cite this article in press as: Jia et al., Extremely Hydrophobic POPs to Access Highly Porous Storage Media and Capturing Agent for Organic Vapors, Chem (2018), https://doi.org/10.1016/j.chempr.2018.10.005

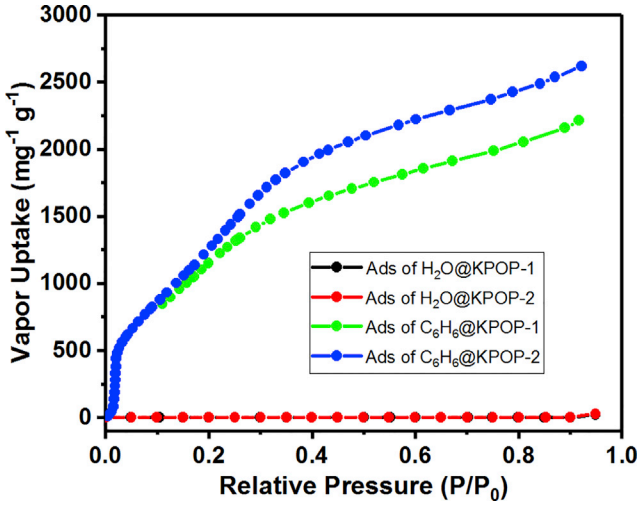

Figure 6. Vapor Sorption Isotherms of KPOP-1 and KPOP-2 (for Benzene and Water) at 25°C (P_0 is the Saturation Vapor Pressure)

P/P_0 = 0.9), respectively. Other hydrophobic organic vapor adsorbates such as hexane and toluene were also tested (Figure S28). The hexane and toluene uptakes for KPOP-1 are 1.7 and 2.1 g^{-1} g^{-1} (25°C, P/P_0 = 0.9), respectively. The corresponding values for KPOP-2 are 2.1 and 2.4 g^{-1} g^{-1} (25°C, P/P_0 = 0.9), respectively. The organic vapor uptake for KPOP-1 and KPOP-2 are pre-eminently higher than most of the other porous materials such as PAF-1[21] and CPOP-9[40] because of their high pore volume and associated hydrophobic surface. The hydrophobicity of the KPOPs was also assessed by carrying out water sorption experiments. It was found that the KPOP-1 and KPOP-2 do not show any water vapor uptake until 85%–90% relative humidity (Figure S27). This clearly attests to the highly hydrophobic character of KPOP-1 and KPOP-2. Such a behavior can be mainly attributed to the presence of hydrophobic phenyl rings and silicone moieties in both KPOP-1 and KPOP-2. These data clearly testify to the distinctive performance of KPOP-1 and KPOP-2 adsorbents for capturing VOCs from atmospheric air.

Considering the outstanding properties of KPOP-1 and KPOP-2 for CH_4 storage and the capture of VOCs, the stability and adsorption recyclability of the two KPOPs were also tested. The study attests to the chemical stability KPOP-2 upon soaking in water, acid solution, and base solution (Figure S42) and shows good adsorption recyclability for C_6H_6 (Figure S43). Notably, KPOP-1 seems to undergo pore size distribution alteration with a higher degree of heterogeneity but without altering the total pore volume after soaking in water, acid, or base (Figure S41). In fact, the N_2 adsorption isotherm at 77 K changed with lower uptake at low relative pressures (at P/P_0 = 0.2, the uptake decreased from 1,250 cm^3 to around 850 cm^3; at P/P_0 = 0.95, the uptake decreased from 1,850 cm^3 to around 1,750 cm^3). This is plausibly due to the occurrence of another amorphous network rearrangement of KPOP-1 with a higher degree of heterogeneity. Both KPOP-1 and KPOP-2 proved highly stable after water vapor adsorption isotherms (Figures S41 and S42).

In conclusion, three highly porous organic polymers were conceived and successfully synthesized according to the MBB strategy. A thorough and unique topological analysis delineated the possible hypothetical structures for KPOP-1, KPOP-2, and KPOP-3. The three KPOPs display high CH_4 uptakes. In particular, KPOP-2 showed

the highest CH_4 storage capacity reported to date, addressing the DOE target at 75 bar and 298 K. More importantly, the unveiled KPOP-2 could be potentially used for non-mobile storage applications with less constrained space requirements. KPOP-2 also shows benchmark O_2 uptake capacity. More interestingly, KPOP-1 and KPOP-2 show highly hydrophobic properties and are can be regarded as promising materials for capturing organic vapors. The findings presented herein represent one important step in the search for synthetic pathways to unlock the discovery of highly porous organic polymers with a high degree of structural uniformity and control. Further studies aiming at exploiting the high hydrophobicity of KPOP-1 and KPOP-2 in various practical applications are under way.

EXPERIMENTAL PROCEDURES

Synthesis of KPOP-1

To a 100-mL flask, 200 mg (0.73 mmol) of $Ni(COD)_2$, 0.9 mL (0.071 mmol) of COD, and 114 mg (0.73 mmol) of 2,2-bipyridyl were dissolved in a mixed dry solvent of DMF/THF (v/v = 10 mL/10 mL) under Ar atmosphere. To this solution, a solution of MBB-1 (100 mg, 0.093 mmol) in 10 mL of dry THF was added dropwise to the solution at room temperature under Ar. The reaction was reacted for 24 hr at room temperature, then 5 mL of 6 M HCl solution was added to the solution and stirred for 8 hr. The white precipitate obtained was filtrated and washed with large amounts of water, methanol, and THF. The product was dried *in vacuo* to give a white powder, KPOP-1 (52 mg, yield = 94%).

Synthesis of KPOP-2

To a 100-mL flask, 200 mg (0.73 mmol) of $Ni(COD)_2$, 0.9 mL (0.071 mmol) of COD, and 114 mg (0.73 mmol) of 2,2-bipyridyl were dissolved in a mixed dry solvent of DMF/THF (v/v = 10 mL/10 mL) under Ar atmosphere. To this solution, a solution of MBB-2 (107 mg, 0.093 mmol) in 10 mL of dry THF was added dropwise to the solution at room temperature under Ar. The reaction was reacted for 24 hr at room temperature, then 5 mL of 6 M HCl solution was added to the solution and stirred for 8 hr. The white precipitate obtained was filtrated and washed with large amounts of water, methanol, and THF. The product was dried *in vacuo* to give a white powder, KPOP-2 (54 mg, yield = 93%).

Synthesis of KPOP-3

To a 100-mL flask, 2.5 g (12.5 mmol) of $Cu(OAc)_2 \cdot 2H_2O$ was dissolved in 100 mL of pyridine at 100°C. To this mixture, a solution of MBB-3 (100 mg, 0.20 mmol) in 5 mL of pyridine was added dropwise to the solution. The reaction was reacted for 1 hr with stirring. The brown precipitate was filtrated and washed with 1 M HCl, ammonium solution, water, methanol, and THF. Thereafter, the products were solvent exchanged by methanol and THF many times and dried under vacuum to yield a brown powder, KPOP-3 (100 mg, yield = 100%).

SUPPLEMENTAL INFORMATION

Supplemental Information includes Supplemental Experimental Procedures, 43 figures, 5 schemes, and 1 table and can be found with this article online at https://doi.org/10.1016/j.chempr.2018.10.005.

ACKNOWLEDGMENTS

Research reported in this publication was fully supported by the King Abdullah University of Science and Technology (KAUST). We thank Daliang Zhang at the core lab of KAUST for the HRTEM characterization.

Please cite this article in press as: Jia et al., Extremely Hydrophobic POPs to Access Highly Porous Storage Media and Capturing Agent for Organic Vapors, Chem (2018), https://doi.org/10.1016/j.chempr.2018.10.005

AUTHOR CONTRIBUTIONS

J.J. synthesized the KPOPs. J.J., K.A., H.J., and M.R.T. characterized the materials. Z.C., Y.B., G.M., and H.A. carried out the adsorption experiments. E.A.-H. carried out the solid-state NMR experiments. J.J. and J.C.-J. performed the organic synthesis. J.J., H.J., Y.B., K.A., and M.E. wrote the manuscript.

DECLARATION OF INTERESTS

The authors declare no competing interests.

Received: June 12, 2018
Revised: July 5, 2018
Accepted: October 11, 2018
Published: November 1, 2018

REFERENCES AND NOTES

1. Li, B., Wen, H.-M., Zhou, W., Xu, J.Q., and Chen, B. (2016). Porous metal-organic frameworks: promising materials for methane storage. Chem *1*, 557–580.

2. Faramawy, S., Zaki, T., and Sakr, A.A.E. (2016). Natural gas origin, composition, and processing: a review. J. Nat. Gas Sci. Eng. *34*, 34–54.

3. Jiang, J.C., Furukawa, H., Zhang, Y.B., and Yaghi, O.M. (2016). High methane storage working capacity in metal-organic frameworks with acrylate links. J. Am. Chem. Soc. *138*, 10244–10251.

4. Peng, Y., Krungleviciute, V., Eryazici, I., Hupp, J.T., Farha, O.K., and Yildirim, T. (2013). Methane storage in metal-organic frameworks: current records, surprise findings, and challenges. J. Am. Chem. Soc. *135*, 11887–11894.

5. Mason, J.A., Veenstra, M., and Long, J.R. (2014). Evaluating metal-organic frameworks for natural gas storage. Chem. Sci. *5*, 32–51.

6. Furukawa, H., Ko, N., Go, Y.B., Aratani, N., Choi, S.B., Choi, E., Yazaydin, A.O., Snurr, R.Q., O'Keeffe, M., Kim, J., et al. (2010). Ultrahigh porosity in metal-organic frameworks. Science *329*, 424–428.

7. Farha, O.K., Eryazici, I., Jeong, N.C., Hauser, B.G., Wilmer, C.E., Sarjeant, A.A., Snurr, R.Q., Nguyen, S.T., Yazaydin, A.O., and Hupp, J.T. (2012). Metal-organic framework materials with ultrahigh surface areas: is the sky the limit? J. Am. Chem. Soc. *134*, 15016–15021.

8. Alezi, D., Belmabkhout, Y., Suyetin, M., Bhatt, P.M., Weseliński, Ł.J., Solovyeva, V., Adil, K., Spanopoulos, I., Trikalitis, P.N., Emwas, A.-H., et al. (2015). MOF crystal chemistry paving the way to gas storage needs: aluminum-based soc-MOF for CH_4, O_2, and CO_2 storage. J. Am. Chem. Soc. *137*, 13308–13318.

9. Howarth, A.J., Peters, A.W., Vermeulen, N.A., Wang, T.C., Hupp, J.T., and Farha, O.K. (2017). Best practices for the synthesis, activation, and characterization of metal-organic frameworks. Chem. Mater. *29*, 26–39.

10. Towsif Abtab, S.M., Alezi, D., Bhatt, P.M., Shkurenko, A., Belmabkhout, Y., Aggarwal, H., Weseliński, Ł.J., Alsadun, N., Samin, U., Hedhili, M.N., et al. (2018). Reticular chemistry in action: a hydrolytically stable MOF capturing twice its weight in adsorbed water. Chem *4*, 94–105.

11. Kang, D.W., Lim, K.S., Lee, K.J., Lee, J.H., Lee, W.R., Song, J.H., Yeom, K.H., Kim, J.Y., and Hong, C.S. (2016). Cost-effective, high-performance porous-organic-polymer conductors functionalized with sulfonic acid groups by direct postsynthetic substitution. Angew. Chem. Int. Ed. *55*, 16123–16126.

12. Van Humbeck, J.F., McDonald, T.M., Jing, X.F., Wiers, B.M., Zhu, G.S., and Long, J.R. (2014). Ammonia capture in porous organic polymers densely functionalized with Bronsted acid groups. J. Am. Chem. Soc. *136*, 2432–2440.

13. Jiang, J.X., Su, F., Trewin, A., Wood, C.D., Campbell, N.L., Niu, H., Dickinson, C., Ganin, A.Y., Rossseinsky, M.J., Khimyak, Y.Z., et al. (2007). Conjugated microporous poly(aryleneethynylene) networks. Angew. Chem. Int. Ed. *119*, 8728–8732.

14. Weber, J., and Thomas, A. (2008). Toward stable interfaces in conjugated polymers: microporous poly(p-phenylene) and poly(phenyleneethynylene) based on a spirobifluorene building block. J. Am. Chem. Soc. *130*, 6334–6335.

15. Chang, Z., Zhang, D.S., Chen, Q., and Bu, X.H. (2013). Microporous organic polymers for gas storage and separation applications. Phys. Chem. Chem. Phys. *15*, 5430–5442.

16. Alkordi, M.H., Haikal, R.R., Hassan, Y.S., Emwas, A.H., and Belmabkhout, Y. (2015). Poly-functional porous-organic polymers to access functionality-CO_2 sorption energetic relationships. J. Mater. Chem. A *3*, 22584–22590.

17. Kaur, P., Hupp, J.T., and Nguyen, S.T. (2011). Porous organic polymers in catalysis: opportunities and challenges. Acs Catal. *1*, 819–835.

18. Das, S., Heasman, P., Ben, T., and Qiu, S.L. (2017). Porous organic materials: strategic design and structure-function correlation. Chem. Rev. *117*, 1515–1563.

19. Cooper, A.I. (2009). Conjugated microporous polymers. Adv. Mater. *21*, 1291–1295.

20. Xu, Y.H., Jin, S.B., Xu, H., Nagai, A., and Jiang, D.L. (2013). Conjugated microporous polymers: design, synthesis and application. Chem. Soc. Rev. *42*, 8012–8031.

21. Ben, T., Ren, H., Ma, S.Q., Cao, D.P., Lan, J.H., Jing, X.F., Wang, W.C., Xu, J., Deng, F., Simmons, J.M., et al. (2009). Targeted synthesis of a porous aromatic framework with high stability and exceptionally high surface area. Angew. Chem. Int. Ed. *48*, 9457–9460.

22. Brunauer, S., Emmett, P.H., and Teller, E. (1938). Adsorption of gases in multimolecular layers. J. Am. Chem. Soc. *60*, 309–319.

23. Yuan, D.Q., Lu, W.G., Zhao, D., and Zhou, H.C. (2011). Highly stable porous polymer networks with exceptionally high gas-uptake capacities. Adv. Mater. *23*, 3723–3725.

24. Eddaoudi, M., Moler, D.B., Li, H., Chen, B., Reineke, T.M., O'Keeffe, M., and Yaghi, O.M. (2001). Modular chemistry: secondary building units as a basis for the design of highly porous and robust metal-organic carboxylate frameworks. Acc. Chem. Res. *34*, 319–330.

25. Chen, Z.J., Weselinski, L.J., Adil, K., Belmabkhout, Y., Shkurenko, A., Jiang, H., Bhatt, P.M., Guillerm, V., Dauzon, E., Xue, D.X., et al. (2017). Applying the power of reticular chemistry to finding the missing alb-MOF platform based on the (6,12)-coordinated edge -transitive net. J. Am. Chem. Soc. *139*, 3265–3274.

26. Zou, X., Ren, H., and Zhu, G. (2013). Topology-directed design of porous organic frameworks and their advanced applications. Chem. Commun. *49*, 3925–3936.

27. Ma, H., Chen, J.-J., Tan, L., Bu, J.-H., Zhu, Y., Tan, B., and Zhang, C. (2016). Nitrogen-rich triptycene-based porous polymer for gas storage and iodine enrichment. ACS Macro Lett. *5*, 1039–1043.

28. Schade, A., Monnereau, L., Muller, T., and Bräse, S. (2014). Hexaphenyl-p-xylene: a rigid pseudo-octahedral core at the service of three-dimensional porous frameworks. ChemPlusChem *79*, 1176–1182.

29. O'Keeffe, M., Peskov, M.A., Ramsden, S.J., and Yaghi, O.M. (2008). The reticular chemistry structure resource (RCSR) database of, and

symbols for, crystal nets. Acc. Chem. Res. *41*, 1782–1789.

30. Li, M., Li, D., O'Keeffe, M., and Yaghi, O.M. (2014). Topological analysis of metal-organic frameworks with polytopic linkers and/or multiple building units and the minimal transitivity principle. Chem. Rev. *114*, 1343–1370.

31. Yamamoto, T., Maruyama, T., Zhou, Z.H., Ito, T., Fukuda, T., Yoneda, Y., Begum, F., Ikeda, T., Sasaki, S., Takezoe, H., et al. (1994). Pi-conjugated poly(pyridine-2,5-diyl), poly(2,2′-bipyridine-5,5′-diyl), and their alkyl derivatives—preparation, linear structure, function as a ligand to form their transition-metal complexes, catalytic reactions, N-type electrically conducting properties, optical-properties, and alignment on substrates. J. Am. Chem. Soc. *116*, 4832–4845.

32. Lu, W.G., Wei, Z.W., Yuan, D.Q., Tian, J., Fordham, S., and Zhou, H.C. (2014). Rational design and synthesis of porous polymer networks: toward high surface area. Chem. Mater. *26*, 4589–4597.

33. Bracco, S., Piga, D., Bassanetti, I., Perego, J., Comotti, A., and Sozzani, P. (2017). Porous 3D polymers for high pressure methane storage and carbon dioxide capture. J. Mater. Chem. A *5*, 10328–10337.

34. Peng, Y., Srinivas, G., Wilmer, C.E., Eryazici, I., Snurr, R.Q., Hupp, J.T., Yildirim, T., and Farha, O.K. (2013). Simultaneously high gravimetric and volumetric methane uptake characteristics of the metal-organic framework NU-111. Chem. Commun. *49*, 2992–2994.

35. Furukawa, H., and Yaghi, O.M. (2009). Storage of hydrogen, methane, and carbon dioxide in highly porous covalent organic frameworks for clean energy applications. J. Am. Chem. Soc. *131*, 8875–8883.

36. Stoeck, U., Krause, S., Bon, V., Senkovska, I., and Kaskel, S. (2012). A highly porous metal-organic framework, constructed from a cuboctahedral super-molecular building block, with exceptionally high methane uptake. Chem. Commun. *48*, 10841–10843.

37. DeCoste, J.B., Weston, M.H., Fuller, P.E., Tovar, T.M., Peterson, G.W., LeVan, M.D., and Farha, O.K. (2014). Metal-organic frameworks for oxygen storage. Angew. Chem. Int. Ed. *53*, 14092–14095.

38. Leemann, M., Eigenberger, G., and STrathmann, H. (1996). Vapour permeation for the recovery of organic solvents from waste air streams: separation capacities and process optimization. J. Membr. Sci *113*, 313–322.

39. Feng, X.S., Sourirajan, S., Tezel, H., and Matsuura, T. (1991). Separation of organic vapor from air by aromatic polyimide membranes. J. Appl. Polym. Sci. *43*, 1071–1079.

40. Chen, Q., Liu, D.P., Zhu, J.H., and Han, B.H. (2014). Mesoporous conjugated polycarbazole with high porosity via structure tuning. Macromolecules *47*, 5926–5931.